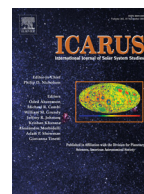




Contents lists available at ScienceDirect

Icarus

journal homepage: [www.elsevier.com/locate/icarus](http://www.elsevier.com/locate/icarus)

# Driven by excess? Climatic implications of new global mapping of near-surface water-equivalent hydrogen on Mars

Asmin V. Pathare<sup>a,\*</sup>, William C. Feldman<sup>a</sup>, Thomas H. Prettyman<sup>a</sup>, Sylvestre Maurice<sup>b</sup>

<sup>a</sup> Planetary Science Institute, Tucson, AZ 85719, United States

<sup>b</sup> Institut de Recherche en Astrophysique et Planétologie, Université Paul Sabatier, Toulouse, France

## ARTICLE INFO

### Article history:

Received 15 May 2017

Revised 25 August 2017

Accepted 26 September 2017

Available online xxx

## ABSTRACT

We present improved Mars Odyssey Neutron Spectrometer (MONS) maps of near-surface Water-Equivalent Hydrogen (WEH) on Mars that have intriguing implications for the global distribution of “excess” ice, which occurs when the mass fraction of water ice exceeds the threshold amount needed to saturate the pore volume in normal soils. We have refined the crossover technique of Feldman et al. (2011) by using spatial deconvolution and Gaussian weighting to create the first globally self-consistent map of WEH. At low latitudes, our new maps indicate that WEH exceeds 15% in several near-equatorial regions, such as Arabia Terra, which has important implications for the types of hydrated minerals present at low latitudes. At high latitudes, we demonstrate that the disparate MONS and Phoenix Robotic Arm (RA) observations of near surface WEH can be reconciled by a three-layer model incorporating dry soil over fully saturated pore ice over pure excess ice: such a three-layer model can also potentially explain the strong anticorrelation of subsurface ice content and ice table depth observed at high latitudes. At moderate latitudes, we show that the distribution of recently formed impact craters is also consistent with our latest MONS results, as both the shallowest ice-exposing crater and deepest non-ice-exposing crater at each impact site are in good agreement with our predictions of near-surface WEH. Overall, we find that our new mapping is consistent with the widespread presence at mid-to-high Martian latitudes of recently deposited shallow excess ice reservoirs that are not yet in equilibrium with the atmosphere.

© 2017 Elsevier Inc. All rights reserved.

## 1. Introduction

There is abundant geomorphic evidence of a large ancient inventory of surface water on Mars, but how much remains extant and where it currently resides is largely unknown: presently, water ice is only stable on the Martian surface near the poles (e.g. Carr, 1996). One of the primary objectives of the Mars Odyssey Neutron Spectrometer (MONS), which measured neutron leakage fluxes from the upper meter of the Martian surface, is to generate global maps of near-surface hydrogen abundance. Although MONS provides an unambiguous indicator of the presence of Water-Equivalent Hydrogen (WEH), quantitative details of its magnitude and burial depth depend on the model of the host regolith utilized to interpret the data. Typically, a two-layer near-surface regolith model is assumed that expresses WEH concentration in terms of an upper layer of weight fraction  $W_{up}$  having thickness  $D$  overlying a semi-infinite lower layer of weight fraction  $W_{dn}$  (e.g. Prettyman et al., 2004). By assuming a constant value of  $W_{up}$ , the

relative proportions of WEH and regolith in the lower layer can be derived, thereby allowing for the creation of global Martian maps of near-surface WEH (Maurice et al., 2011).

Here, we present improved global MONS-derived maps of near-surface WEH, based on the “crossover” technique developed by Feldman et al. (2011), which self-consistently determines – entirely from MONS neutron flux observations – the WEH content of the upper layer ( $W_{up}$ ). We have refined the Feldman et al. (2011) crossover technique by utilizing spatial deconvolution of MONS counting rate data (e.g. Prettyman et al., 2009) and employing a Gaussian-weighted least squares fit parameterization of the deconvolved MONS counting rates to improve determinations of  $W_{up}$ . These enhancements have allowed us to create **the most definitive global map to date of the vertical distribution of WEH in the upper meter of the Martian surface** – which we will utilize to inform fundamental questions related to the global distribution and long-term stability of near-surface water ice and hydrates on Mars.

## 2. Previous MONS mapping

The first Mars Odyssey Neutron Spectrometer results were reported by Feldman et al. (2002), who from just one month of

\* Corresponding author at: Planetary Science Institute, 1700 E. Fort Lowell, Suite 106, Tucson, AZ 85719, United States.

E-mail address: [pathare@psi.edu](mailto:pathare@psi.edu) (A.V. Pathare).

<https://doi.org/10.1016/j.icarus.2017.09.031>

0019-1035/© 2017 Elsevier Inc. All rights reserved.

MONS data found evidence for buried water ice at high latitudes (poleward of  $\pm 60^\circ$ ) tens of cm below the surface, as well as lower-latitude deposits (in regions such as Arabia Terra) that are consistent with chemically or physically bound subsurface  $\text{H}_2\text{O}$  and/or OH. Feldman et al. (2003a) mapped the global distribution of near-surface WEH, assuming a single uniform layer, and found a total inventory of near-surface hydrogen in the upper meter of the Martian surface equivalent to a 13-cm thick global layer of  $\text{H}_2\text{O}$ . Feldman et al. (2003b) calculated MONS-derived  $\text{CO}_2$  frost cap thickness variations during northern winter and spring, obtaining values that were significantly lower than those inferred from Mars Orbiter Laser Altimeter (MOLA) measurements and more consistent with Global Circulation Model (GCM) estimates. This detailed analysis of  $\text{CO}_2$  frost thickness provided an essential calibration (see Fig. 4 in Feldman et al., 2003b) for the Monte Carlo N-Particle eXtended (MCNPX) simulation code more fully described in Prettyman et al. (2004) that is used to convert top-of-the-atmosphere neutron current MONS observations to estimates of (sub)surface hydrogen composition. Prettyman et al. (2004), which focused on MONS results for high southern latitudes, also presented the first two-layer model (described by three independent attributes:  $W_{\text{up}}$ ,  $W_{\text{dn}}$ , and  $D$ ) of near-surface hydrogen content.

Feldman et al. (2004a) refined the single layer (i.e.,  $D = 0$ ) global MONS mapping of Feldman et al. (2003a) by incorporating a two-layer surface model (assuming  $W_{\text{up}} = 2\%$ ) equatorward of  $\pm 45^\circ$ , where predicted WEH contents ranged from 2% to 10% (by weight, which is how all  $\text{WEH}/W_{\text{up}}/W_{\text{dn}}$  values are expressed in this paper). Feldman et al. (2007, 2008a) applied the two-layer surface model (for  $W_{\text{up}} = 1\%$ ) to high northern and southern Martian latitudes, finding a strong anti-correlation between lower layer WEH content  $W_{\text{dn}}$  and apparent depth  $D$ , as well as north-to-south asymmetries in the high latitude WEH distribution. In order to study the hydrogen content of sand dunes within Olympia Undae, Feldman et al. (2008b) applied deconvolution techniques to MONS neutron flux data; similarly, Prettyman et al. (2009) utilized Jansson's algorithm to deconvolve MONS epithermal counting rates to better characterize the evolution of Martian seasonal caps. Diez et al. (2008) explored the effects of compositional variations upon MONS-derived WEH maps by assessing the range of macroscopic absorption cross sections measured in situ by the Mars Exploration Rovers Spirit and Opportunity, and found that an average value ("Composition 21") generated from soils at five Mars mission landing sites (Viking 1, Viking 2, Pathfinder, Spirit, and Opportunity) minimized MONS mapping variance associated with compositional uncertainties.

Maurice et al. (2011) developed new data reduction and analysis techniques for the raw MONS data collected by the four Prism sensors, thereby generating thermal, epithermal, and fast neutron counting rates – which represent the three primary MONS-derived data sets – with significantly reduced counting-rate variances (Maurice et al., 2011). In theory, since there are three MONS-derived measurables (thermal, epithermal, and fast neutron counting rates), and three MCNPX model unknowns ( $W_{\text{up}}$ ,  $D$ , and  $W_{\text{dn}}$ ), it should be possible to derive a unique solution for the vertical distribution of WEH. However, the actual response of the fast neutrons to surficial hydrogen is extremely similar to that of the epithermals, making it difficult to disentangle the two data sets (Feldman et al., 2002; Prettyman et al., 2004). Therefore, most previous workers assumed a constant value for  $W_{\text{up}}$ , and then used thermal and epithermal counting rates to produce global maps of Martian  $D$  and  $W_{\text{dn}}$  (e.g. Feldman et al., 2004a, 2007, 2008a; Maurice et al., 2011).

Feldman et al. (2011) devised a crossover technique that self-consistently determines  $W_{\text{up}}$  from the MONS fast and epithermal neutron counting rates. Feldman et al. (2011) generated the first-ever global map of  $W_{\text{up}}$  by applying their crossover technique

to MONS fast and epithermal counting rates from large sliding 1800-km diameter Regions of Interest (ROIs). However, their initial crossover-derived  $W_{\text{up}}$  mapping (see Fig. 7 of Feldman et al., 2011) contained obvious inconsistencies: for example, several regions at lower latitudes were mapped as having negative values of  $W_{\text{up}}$ , which is of course unphysical.

In this work, we improve upon previous MONS-derived global mapping of  $W_{\text{dn}}$ ,  $D$ , and  $W_{\text{up}}$  (Maurice et al., 2011; Feldman et al., 2011) in two ways. First, we apply an iterated spherical harmonic expansion of the latitude-longitude count-rate matrix to the Maurice et al. (2011) global mapping of epithermal, thermal, and fast neutron count rates using a newly-developed deconvolution algorithm (described in the Appendix). Secondly, we improve upon the Feldman et al. (2011) crossover technique to calculate  $W_{\text{up}}$ , which utilized unweighted sliding 1800-km ROIs, by incorporating a Gaussian-weighted least squares fit parameterization. Since we self-consistently derive  $W_{\text{up}}$  directly from MONS data (instead of assuming a constant value like most previous workers), our resulting  $W_{\text{up}}$ -dependent maps of  $W_{\text{dn}}$  and  $D$  represent the most definitive global mapping to date of the vertical distribution of WEH in the upper meter of the Martian surface.

### 3. Methodology

#### 3.1. Neutron count rates

The starting point for our global mapping of near-surface WEH on Mars is the apportionment by Maurice et al. (2011) of epithermal, thermal, and fast neutron count rates to equal-area grids equivalent to  $1^\circ$  of latitude  $\times$   $1^\circ$  of longitude at the equator. The comprehensive analysis of Maurice et al. (2011) included MONS observations of frost-free Martian surfaces, beginning in February of 2002 with the attainment of a near-polar ( $\sim 93^\circ$  inclination) 400 km altitude circular orbit and extending for approximately 3.5 Martian years through July of 2009. The accumulation time for individual data samples is 1 s, and the total number of samples in these data sets is sufficiently large that uncertainties in each of the count-rate entries in the count-rate arrays are limited by systematic effects, not statistics (Maurice et al., 2011). Undeconvolved global maps of epithermal, thermal, and fast neutron count rates are shown in Figs. 1a, 2a, and 3a, respectively (note that these global maps have been generated from the same epithermal/thermal/fast neutron count rate data sets utilized to produce the global maps shown in Figs. 17, 25 and 30 of Maurice et al., 2011).

In order to improve upon the Maurice et al. (2011) global mapping of epithermal, thermal, and fast neutron count rates, we spatially deconvolved all three of these MONS data sets. Whereas previously we have utilized the Pixon method (Puetter, 1995; Feldman et al., 2008a) and an iterated Jansson algorithm (Jansson, 1997; Prettyman et al., 2009), in this work we implement a new deconvolution methodology (detailed in the Appendix) involving a tesseral spherical harmonics (TSH) expansion (a.k.a. "real" spherical harmonics) of the latitude-longitude count rate matrices. As discussed below, we find that a deconvolution solution utilizing a TSH order of  $\{N = 16\}$  provides the most physically credible representation of the MONS data (where "order" is defined in Appendix Eq. (A2)). Our resulting deconvolved  $\{N = 16\}$  global maps of epithermal, thermal, and fast neutron count rates are shown in Figs. 1b, 2b, and 3b, respectively.

##### 3.1.1. Epithermal neutron counting rates

$C_E$  can be calculated directly from the MONS downward-facing Prism-1 sensor (Feldman et al., 2003b). The global maps of undeconvolved (Fig. 1a) and  $\{N = 16\}$  deconvolved (Fig. 1b) epithermal neutron count rates are fairly similar at lower latitudes: the

Download English Version:

<https://daneshyari.com/en/article/8134661>

Download Persian Version:

<https://daneshyari.com/article/8134661>

[Daneshyari.com](https://daneshyari.com)